

Treatment planning validation for symmetric and asymmetric motorized wedged fields

Tamer Dawod

Department of Clinical Oncology and Nuclear Medicine, Faculty of Medicine, Mansoura University, Mansoura, Egypt

Received October 24, 2014; Revised December 25, 2014; Accepted January 05, 2015; Published Online January 20, 2015

Technical Report

Abstract

Purpose: Wedged beam are often used in clinical radiotherapy to compensate missing tissues and dose gradients. The Elekta Precise linear accelerator supports an internal motorized wedge, which is a single large, physical wedge on a motorized carriage. In this study, the dosimetric performance of Elekta precise three dimensional treatment planning system (3DTPS) is evaluated by comparing the calculated and measured doses. **Methods:** The calculations were performed by the 3DTPS for symmetric as well as asymmetric fields in a source to skin distance (SSD) setup at the depth of maximum dose (d_{max}) as well as at 5, 10, and 20 cm depths in water phantom using 60° motorized wedges for field sizes of 4×4 , 10×10 , and 20×20 cm² for 6 and 15 MV photon beams. Measurements were produced by Elekta Precise linear accelerator using 0.125 cc volume ionization chamber. **Results:** Good agreement between the measured and calculated isodose lines were found, with the maximum difference not exceed 5%. The difference between the calculated and measured data increases as the field size decreases, and the deviation in symmetric setting was less than that of asymmetric setting. The increase in wedge angle led to increase in the difference between calculated and measured data. **Conclusion:** The results from this study showed that the accuracy of Elekta Precise 3DTPS used with the motorized wedges for symmetric and asymmetric fields is adequate for the clinical applications under the studied experimental conditions.

Keywords: Radiotherapy; Motorized Wedge; Linear Accelerator

Introduction

Radiation therapy is the method for the treatment of cancer in which about 60% of patients require radiotherapy as curative or palliative intent.¹ The radiation dose must be delivered within $\pm 5\%$ of the prescribed dose.^{2,3} In computerized treatment planning system TPS, the most important software component is the dose calculation algorithm which is responsible for the precise delivery of dose to target volume, and it may be linked to the calculation of monitor units (MUs). Three-dimensional conformal radiotherapy (3D-CRT) uses certain beam shaping devices in order to confirm the shape of beam to the target area of the patient. The target of such technique is to deliver high doses of energetic radiations to the tumor and reduce the exposure of normal tissues.^{4,5}

Commissioning of the dose calculation algorithms of a treatment planning system is generally performed: (i) by entering basic beam data into the system according to the methods and requirements described in the user's manual of the system; and (ii) by comparing the results of dose calculations with the entered data and with data that were measured specially for this purpose.⁶ Differences between calcu-

lated and actual dose values may be encountered, partly due to uncertainties in the measured data, and partly due to imperfect beam modeling.⁷ A number of complex irradiation techniques apply wedged asymmetric high-energy photon beams. The reason for using these asymmetric fields is that the patient set-up becomes more accurate because the isocenter does not have to be shifted, for instance if abutting fields are applied.⁸

Wedges are commonly used as beam-modifying devices in radiation therapy to optimize the target volume dose distribution.^{9,10} Physical wedges have been used for many decades. Further developments in the head design have brought the concept of "universal wedges (UW) and motorized wedge (MW)". MW is a single physical wedge (60°) which could generate desired angle (0 to 60°) with the combination of open and wedged beam.¹¹ Venselaar *et al.*⁷ recently showed for a number of commercial treatment planning systems, that the algorithms for calculating monitor units (MUs) in wedged asymmetric fields have their limitations. Deviations up to 13% between the calculated and measured dose values were observed and had different magnitudes at the thin and

thick side of the wedge. Considering the deviations that are acceptable in these types of dose calculations it is important to have an independent MU calculation, to verify the clinically applied MU values. There are several papers reporting the results of wedge beam profile measurements from physical, virtual and dynamic filters, using different dosimeters such as diode¹², ionization chamber¹³⁻¹⁵, and film.¹⁵ The aim of this study was therefore to evaluate Elekta Precise three dimensional treatment planning system (3DTPS) precision in modeling dose distributions by comparing calculated with measured dose for (symmetric and asymmetric) motorized wedged fields by using 60° to check if the planning system calculate the dose correct or not.

Methods and Materials

Beam data were obtained at an Elekta precise linear accelerator for 6 and 15 MV photon beams available at Clinical Oncology and Nuclear Medicine Department, Mansoura University. The percentage depth dose (PDD) and profile measurements were measured at predefined depths in water phantom with a PTW dosimetry system with two semiflex (0.125 cc) ionization chamber. The chamber was mounted in a holder, placed in a 50 cm × 50 cm × 50 cm PTW three dimensional water phantom. The water surface was leveled at Source to Skin Distance SSD of 100 cm. The gantry of the treatment unit was set to 0°. The linac was set to deliver 700 monitor units (MUs) per minute. To reduce the variability of working conditions, the dosimetry measurements were performed in a single session. The MW provides a 60° nominal wedge angle. The maximum field size covered by the MW is 25 cm, alternately; it can be moved in and out of the radiation fields. It consists of a 60-degree wedge mounted in the asymmetric collimator below the lead leaves and above the tungsten trimmer bars. When the collimator is at zero angle position, the MW is oriented with the thin edge directed to the left when facing the gantry. In this work we used 0.125 cc volume of ionization chamber for measuring dose and VeriSoft software (Version 4) for the validation of the dose.

The dose distributions were calculated by Elekta 3DTPS. The MW with symmetric and asymmetric fields for 4 cm × 4 cm and 10 cm × 10 cm, 20 cm × 20 cm, the fields were shown in **Table 1**. The beam profile for the scanned fields were measured at depths of d_{max} , 5, 10, 20 cm with source to surface distance (SSD) of 100 cm as shown in **Figure 1** for field size 20 × 20. Calculations were performed in a phantom created by Elekta precise 3D planning a homogeneous density of 1 g/cm³. The dose was calculated for 6 and 15 MV photon beams at each depth.

In order to compare calculated and measured doses, we used PTW VeriSoft software to verify the treatment plan by comparing calculated data to its corresponding measured data in the phantom. According to the tolerance values for homogeneous simple fields, the penumbra region should be

within 2 mm or 10%.⁶ By just studying the profiles by visual inspection, it is hard to say, especially in the z-direction in the penumbra region, if the result is within the tolerance. A gamma evaluation with 3% and 3 mm criteria, revealing that it is only in the penumbra region that acceptance fails. The colors of the palette range are set to be green for 100% ($\gamma = 1$), and accepted regions are green and most yellow. Regions that fail are shown in red. The gamma evaluation method is not a good tool for evaluation of low dose regions, where the calculation can fail though it is within the set criteria. For example, if we are comparing two dose points of 4% and 1% dose, and the dose criteria is set to be 2%, this will lead to a gamma value larger than 1 ((4%-1%)/2%). The 3% dose difference can still be within acceptable tolerances but the gamma calculation fails.

TABLE 1: Symmetric and asymmetric field sizes for jaws direction.

Field Size	No of Fields	Jaws Direction			
		X1	X2	Y1	Y2
4 cm × 4 cm	1	2	2	1	3
	2	2	2	2	2
	3	2	2	3	1
10cm × 10 cm	1	5	5	2	8
	2	5	5	4	6
	3	5	5	5	5
	4	5	5	6	4
	5	5	5	8	2
20 cm × 20cm	1	10	10	5	15
	2	10	10	10	10
	3	10	10	15	5

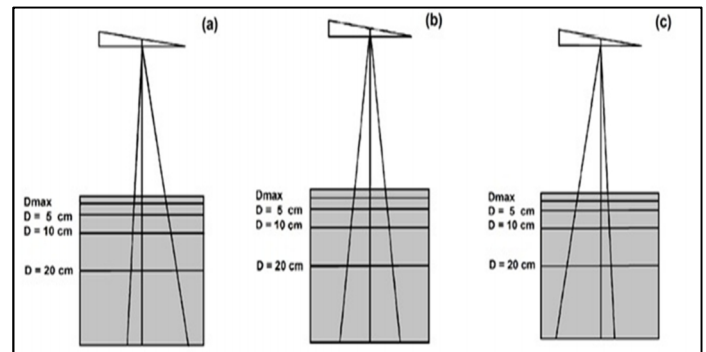


FIG. 1: View of the beam setup showing the depths of measurement field size 20 × 20 cm², 6MV, SSD = 100 cm. In the asymmetrical (X1 = 10, X2 = 10, Y1 = 5, Y2 = 15); (b) in the symmetrical setting (X1 = 10, X2 = 10, Y1 = 10, Y2 = 10); and (c) in the asymmetrical setting (X1 = 10, X2 = 10, Y1 = 15, Y2 = 5).

Results

In radiation treatment planning, the desired wedged dose distribution is obtained by the proper combination of wedged and unwedged treatment.¹⁶ Measured data with 6 and 15 MV for 4, 10, and 20 cm field sizes were compared with data from TPS for motorized wedge with angle 60°. The

statistical analysis was performed using the PTW-VeriSoft program to evaluate the differences between the data.

Twenty two symmetric and asymmetric fields with 6 and 15 MV energy were used for comparison and verification. **Figure 1** shows the view of the beam setup showing the field sizes of measurement in the (a) asymmetrical setting ($X1 = 5$, $X2 = 5$, $Y1 = 2.5$, $Y2 = 7.5$), (b) symmetrical setting ($X1 = 5$, $X2 = 5$, $Y1 = 5$, $Y2 = 5$), and (c) asymmetrical setting ($X1 = 5$, $X2 = 5$, $Y1 = 7.5$, $Y2 = 2.5$).

For the first field size shown in **Figure 2**, the measured and calculated beam isodose results for motorized wedge filters are presented for field size 4×4 cm². The result of the comparison was displayed for both images using the gamma method. **Table 2** represents the difference between measured dose and calculated dose at different isodose lines for symmetric and asymmetric fields for the dual energy for wedge angles 60°. **Figure 2 and 3** show the comparison of the dose distribution by the gamma method for energies, different field size. It defines a percentage difference between the measured and the calculated formula for the difference matrix with the "Local Percentage Difference" method:

$$D = \frac{V(i,j) - R(i,j)}{R(i,j)} \times 100\%$$

$V(i, j)$ value at the point (i, j) of the comparative matrix

$R(i, j)$ value at the point (i, j) of the reference matrix

This part included two symmetric fields and four asymmetric fields. The data showed that the differences between the measured and the calculated distributions for all isodose lines, symmetric and asymmetric, did not exceed 5% within the distance of 3 mm. The maximum difference was found at asymmetric field size ($X = 4$ and $Y1 = 1$, $Y2 = 3$) and the difference between measured and calculated was up to 5% for 6 MV.

For the second field size 10×10 cm² shown in **Figures 3, 4**, and **Table 3**, it included two symmetric fields and eight asymmetric fields. The data showed that the differences between the measured and the calculated distributions for all isodose lines, symmetric, and asymmetric, did not exceed 4% within the distance of 3 mm. The maximum difference was found at asymmetric field size ($X = 10$ & $Y1 = 2$, $Y2 = 8$), and the difference between measured and calculated was up to 4% for 6 MV.

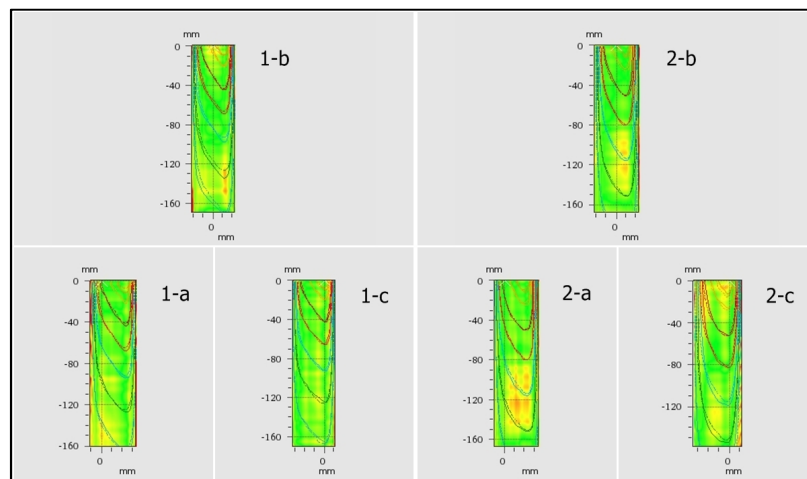


FIG. 2: Gamma distribution for different field using the full area integrated algorithm for 60 degree motorized wedge (MW), for 6 and 15 MV and field size 4×4 cm². The green color indicates regions where gamma ≤ 1 ; and red indicates gamma > 1 (individual criteria: $\Delta\%D = 3\%$, DTA = 3 mm). (a) Asymmetric setting ($X = 4$, $Y1 = 1$, $Y2 = 3$); (b) Symmetric setting ($X = 4$, $Y = 4$); (c) Asymmetric setting ($X = 4$, $Y1 = 3$, $Y2 = 1$).

TABLE 2: Difference between measured dose and calculated dose at different isodose lines for symmetric and asymmetric fields for field size 4×4 cm² at 6 and 15MV using motorized wedge with angle 60.

		Gamma Index (3mm)			
	Field Size (cm ²)	Evaluated Dose Points	Passed	Failed	Result
Wedge 60, 6MV	(1 × 3)		95.20%	4.80%	95.20%
	(2 × 2)	100%	98.40%	1.60%	98.40%
	(3 × 1)		96.90%	3%	96.90%
Wedge 60, 15MV	(1 × 3)		97.20%	2.80%	97.20%
	(2 × 2)	100%	98.40%	1.60%	98.40%
	(3 × 1)		97.40%	2.60%	97.40%

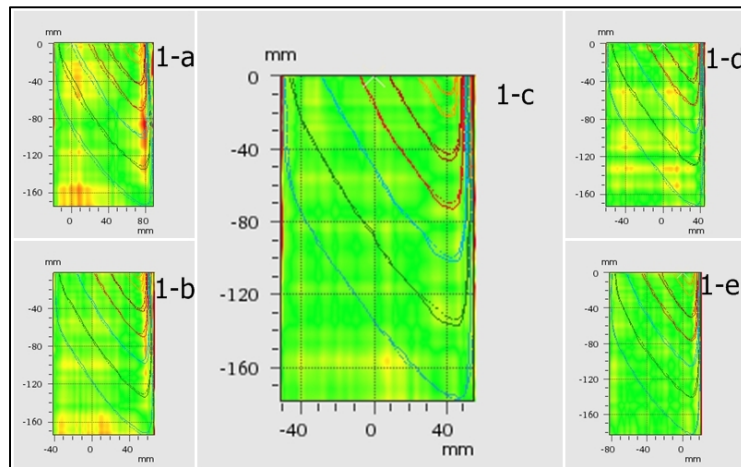


FIG. 3: Gamma distribution for different field using the full area integrated algorithm for 60 degrees motorized wedge (MW), for 6 MV and field size $10 \times 10\text{cm}^2$. The green color indicates regions where $\gamma \leq 1$; and red indicates $\gamma > 1$ (individual criteria: $\Delta\%D = 3\%$, $DTA = 3\text{mm}$). (a) Asymmetric setting ($X = 10$, $Y1 = 2$, $Y2 = 8$); (b) Asymmetric setting ($X = 10$, $Y1 = 4$, $Y2 = 6$); (c) Symmetric setting ($X = 10$, $Y = 10$); (d) Asymmetric setting ($X = 10$, $Y1 = 6$, $Y2 = 4$); and (e) Asymmetric setting ($X = 10$, $Y1 = 8$, $Y2 = 2$).

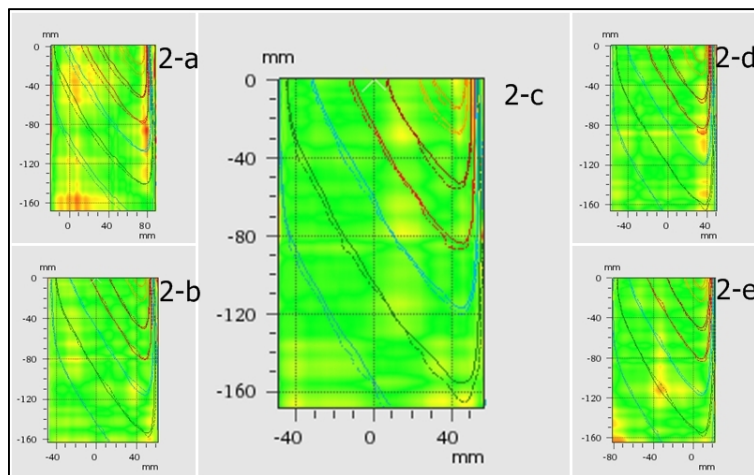


FIG. 4: Gamma distribution for different field using the full area integrated algorithm for 60 degrees motorized wedge (MW), for 15 MV and field size $10 \times 10\text{cm}^2$. The green color indicates regions where $\gamma \leq 1$; and red indicates $\gamma > 1$ (individual criteria: $\Delta\%D = 3\%$, $DTA = 3\text{mm}$). (a) Asymmetric setting ($X = 10$, $Y1 = 2$, $Y2 = 8$); (b) Asymmetric setting ($X = 10$, $Y1 = 4$, $Y2 = 6$); (c) Symmetric setting ($X = 10$, $Y = 10$); (d) Asymmetric setting ($X = 10$, $Y1 = 6$, $Y2 = 4$); and (e) Asymmetric setting ($X = 10$, $Y1 = 8$, $Y2 = 2$).

TABLE 3: Difference between measured dose and calculated dose at different isodose lines for symmetric and asymmetric fields for field size $10 \times 10\text{cm}^2$ at the 6 and 15MV using motorized wedge with angle 60.

Gamma Index (3mm)					
	Field size (cm^2)	Evaluated Dose Points	Passed	Failed	Result
Wedge 60, 6MV	(2×8)	100%	96.50%	3.50%	96.50%
	(4×6)		98.10%	1.90%	98.10%
	(5×5)		98.70%	1%	98.70%
	(6×4)		98.50%	2%	98.50%
	(8×2)		98.40%	2%	98.40%
Wedge 60, 15MV	(2×8)	100%	98.90%	1.10%	98.90%
	(4×6)		99.10%	0.90%	99.10%
	(5×5)		99.50%	1%	99.50%
	(6×4)		99.40%	1%	99.40%
	(8×2)		99.40%	1%	99.40%

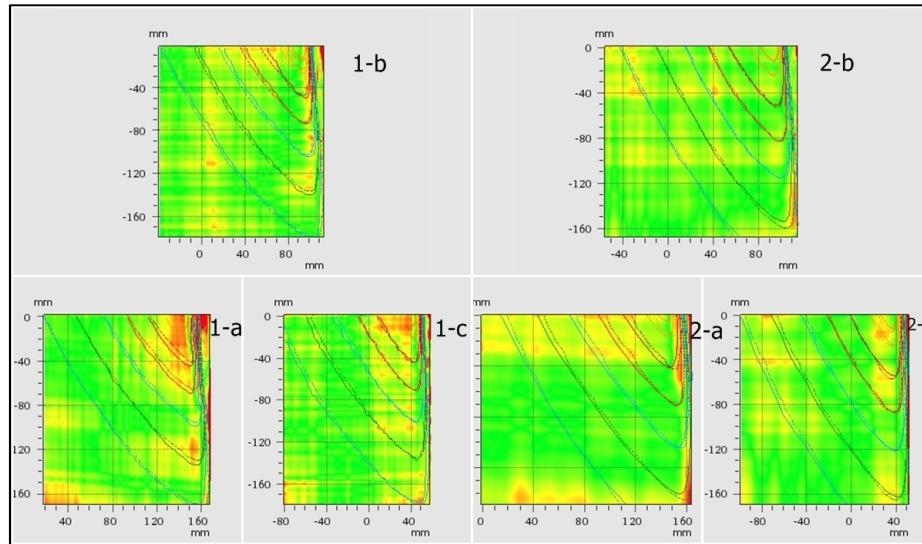


FIG. 5: Gamma distribution for different field using the full area integrated algorithm for 60 degrees motorized wedge (MW), for 6 and 15 MV and field size $20 \times 20 \text{ cm}^2$. a) Asymmetric setting ($X = 20$, $Y1 = 5$, $Y2 = 15$); (b) Symmetric setting ($X = 20$, $Y = 20$); (c) Asymmetric setting ($X = 20$, $Y1 = 15$, $Y2 = 5$).

TABLE 4: Difference between measured dose and calculated dose at different isodose lines for symmetric and asymmetric fields for field size $20 \times 20 \text{ cm}^2$ at the 6 and 15MV using motorized wedge with angle 60.

Gamma Index (3mm)					
	Field Size (cm^2)	Evaluated Dose Points	Passed	Failed	Result
Wedge 60, 6MV	(5×15)		95.30%	4.70%	95.30%
	(10×10)	100%	98.80%	1.20%	98.80%
	(15×5)		97.90%	2%	97.90%
Wedge 60, 15MV	(5×15)		98.70%	1.30%	98.70%
	(10×10)	100%	99.10%	0.90%	99.10%
	(15×5)		98.50%	1.50%	98.50%

For the third field size $20 \times 20 \text{ cm}^2$ shown in **Figure 5** and **Table 4**, it included two symmetric fields and four asymmetric fields. The data showed that the differences between the measured and the calculated distributions for all isodose lines, symmetric and asymmetric, dose not exceeded 5% within the distance of 3 mm. the maximum difference found at asymmetric field size ($X = 20$ & $Y1 = 5$, $Y2 = 15$), the difference between measured and calculated up to 5% for 6 MV.

From all data presented in this study, we showed that there is good agreement between measured and calculated isodose lines, and the maximum difference did not exceed 5%. Additionally, the difference decreased as the energy increased, and the difference between measured and calculated decreased as the field size increased toward the thin edge of the field. In general, the wedge filter alters the beam quality by preferentially attenuating the lower energy photons (beam hardening) and, to a lesser extent, by Compton scattering, which results in energy degradation (beam softening). For x-rays, there can be some beam hardening, and consequently, the depth dose distribution can be somewhat altered,

especially at large depths.¹⁷⁻¹⁹ When a field is collimated asymmetrically, one needs to take into account changes in the collimator scatter, phantom scatter, and off-axis beam quality. The latter effect arises as a consequence of using beam-flattening filters (thicker in the middle and thinner in the periphery), which results in greater beam hardening close to the central axis compared with the periphery of the beam.¹⁹

Discussion

Published data for the TPS dose calculations present significant variation. The first criteria published by Van Dyk *et al.*²⁰ are characterized by increased tolerance limits due to the fact that most of the TPS were using two dimensional algorithms at the time. The recommendations of AAPM TG53 report in 1998 by Fraass *et al.*²¹, and Venselaar *et al.*⁷ showed that the algorithms for calculating monitor units for wedged asymmetric have their limitation. Deviation up to 13 % between measured and calculated dose were observed under the thick and the thin end of the wedge are generally

more strict, but realistic for a properly functioning dose calculation algorithm. When the complexity of the geometry increases, however, tolerance limits may have to be less strict relative to beam modeling geometry.²²

The highest difference of our results is lower than Venselaar *et al.*⁷ and lower than Caprile *et al.*²³, and reaches up to 28.5% for pencil-beam convolution (PBC) for field size 20 × 20. The disagreement regions correspond to the edge of the field where the penumbra is not well modeled. The results showed that the comparison between the measured and calculated motorized wedge depends strongly on field size. The difference between the calculated and measured data increases as the field size decreases, and the deviation in symmetric setting was less than that of asymmetric setting. The results also indicated that the quality of the radiation beam plays a significant role in the dose calculation. With every changing wedge angle, the hardening and softening of the beam varies, indicating the vital role of the wedge factor dependence of the dose. Thus, the quality of the beam itself is of significant importance in the dose precision. These results agreed with Muhammad Maqbool *et al.*²⁴ Our study showed that an increase in wedge angle led to increase in the difference, and this is an agreement with Nath *et al.*²⁵, Pasquino *et al.*²⁶ and Momennezhad *et al.*²⁷ In this study, dose calculations were performed in Elekta 3DTPS, and it is recommended to carry out similar studies for other dose calculation algorithms such as collapsed cone convolution superposition (CCCS) algorithm²⁸, pencil beam convolution (PBC)²⁹, Acuros XB³⁰ and anisotropic analytical algorithm (AAA)^{29,31}.

Conclusion

We have presented the radiation beam profiles using motorized wedge filters for 6 and 15 MV photon beams from Elekta Precise Linac. The measurements were done for symmetric and asymmetric fields. The results presented in this study showed that the accuracy of Elekta Precise 3DTPS used with the motorized wedges for symmetric and asymmetric fields is adequate for the clinical applications under the studied experimental conditions.

Conflict of interest

The authors declare that they have no conflicts of interest. The authors alone are responsible for the content and writing of the paper.

References

1. Ravichandran R. Has the time come for doing away with Cobalt-60 teletherapy for cancer treatments. *J Med Phys* 2009; **34**:63-5.
2. Alam R, Ibbott GS, Pourang R, Nath R. Application of AAPM Radiation Therapy Committee Task Group 23 test package for comparison of two treatment planning systems for photon external beam radiotherapy. *Med Phys* 1997; **24**:2043-54.
3. Murugan A, Valas XS, Thayalan K, Ramasubramanian V. Dosimetric evaluation of a three-dimensional treatment planning system. *J Med Phys* 2011; **36**:15-21.
4. Tome WA, Meeks SL, Buatti JM, *et al.* A high-precision system for conformal intracranial radiotherapy. *Int J Radiat Oncol Biol Phys* 2000; **47**:1137-43.
5. Shahid M, Rafique A, Sabir R, *et al.* Dosimetric evaluation of treatment planning using dynamic and physical wedges: a comparative study. *Peak Journal of Medicine and Medical Science* 2013; **1**:39-48.
6. Venselaar J, Welleweerd H. Application of a test package in an intercomparison of the photon dose calculation performance of treatment planning systems used in a clinical setting. *Radiother Oncol* 2001; **60**:203-13.
7. Venselaar J, Welleweerd H, Mijnheer B. Tolerances for the accuracy of photon beam dose calculations of treatment planning systems. *Radiother Oncol* 2001; **60**:191-201.
8. Smulders B, Bruinvis IA, Mijnheer BJ. Monitor unit calculations for wedged asymmetric photon beams. *Phys Med Biol* 2002; **47**:2013-30.
9. Popescu A, Lai K, Singer K, Phillips M. Wedge factor dependence with depth, field size, and nominal distance--a general computational rule. *Med Phys* 1999; **26**:541-9.
10. Ahmad M, Hussain A, Muhammad W, *et al.* Studying wedge factors and beam profiles for physical and enhanced dynamic wedges. *J Med Phys* 2010; **35**:33-41.
11. Kinhikar RA, Sharma S, Upreti R, *et al.* Characterizing and configuring motorized wedge for a new generation telecobalt machine in a treatment planning system. *J Med Phys* 2007; **32**:29-33.
12. Spezi E, Lewis DG, Smith CW. Monte Carlo simulation and dosimetric verification of radiotherapy beam modifiers. *Phys Med Biol* 2001; **46**:3007-29.
13. Miften M, Zhu XR, Takahashi K, *et al.* Implementation and verification of virtual wedge in a three-dimensional radiotherapy planning system. *Med Phys* 2000; **27**:1635-43.
14. Liu HH, Lief EP, McCullough EC. Measuring dose distributions for enhanced dynamic wedges using a multichamber detector array. *Med Phys* 1997; **24**:1515-9.
15. Bidmead AM, Garton AJ, Childs PJ. Beam data measurements for dynamic wedges on Varian 600C

- (6 MV) and 2100C (6 and 10 MV) linear accelerators. *Phys Med Biol* 1995; **40**:393-411.
16. Halperin EC, Perez CA, Brady LW. Perez and Brady's Principles and Practice of Radiation Oncology, 5th Edition. Lippincott Williams & Wilkins 2007.
 17. Mayles P, Nahum A, Rosenwald JC. Handbook of radiotherapy physics: theory and practice. Taylor & Francis Group, LLC 2007.
 18. Pokharel S. Dosimetric impact of mixed-energy volumetric modulated arc therapy plans for high-risk prostate cancer. *Int J Cancer Ther Oncol* 2013; **1**:01011.
 19. Khan FM. The Physics of Radiation Therapy. 4th Edition. Williams and Wilkins, London. 2010.
 20. Van Dyk J, Barnett R, Cygler J, Shragge P. Commissioning and quality assurance of treatment planning computers. *Int J Radiat Oncol Biol Phys* 1993; **26**:261-73.
 21. Fraass B, Doppke K, Hunt M, *et al*. American Association of Physicists in Medicine Radiation Therapy Committee Task Group 53: quality assurance for clinical radiotherapy treatment planning. *Med Phys* 1998; **25**:1773-829.
 22. Anjum MN, Qadir A, Afzal M. Dosimetric evaluation of a treatment planning system using pencil beam convolution algorithm for enhanced dynamic wedges with symmetric and asymmetric fields. *Iran J Radiat Res* 2008; **5**: 169-74.
 23. Caprile PF, Venencia CD, Besa P. Comparison between measured and calculated dynamic wedge dose distributions using the anisotropic analytic algorithm and pencil-beam convolution. *J Appl Clin Med Phys* 2006; **8**:47-54.
 24. Muhammad W, Maqbool M, Shahid M, *et al*. Technical note: Accuracy checks of physical beam modifier factors algorithm used in computerized treatment planning system for a 15 MV photon beam. *Rep Pract Oncol Radiother* 2009; **14**: 214-20.
 25. Nath R, Biggs PJ, Bova FJ, *et al*. AAPM code of practice for radiotherapy accelerators: report of AAPM Radiation Therapy Task Group No. 45. *Med Phys* 1994; **21**:1093-121.
 26. Pasquino M, Casanova Borca V, Tofani S, Ozzello F. Verification of Varian Enhanced Dynamic Wedge implementation in masterplan treatment planning system. *J Appl Clin Med Phys* 2009; **10**:2867.
 27. Momennezhad M, Bahreyni Toosi MT, Sadeghi R, *et al*. A Monte Carlo simulation and dosimetric verification of physical wedges used in radiation Therapy. *Iran J Radiat Res* 2010; **7**: 223-7.
 28. Oyewale S. Dose prediction accuracy of collapsed cone convolution superposition algorithm in a multi-layer inhomogenous phantom. *Int J Cancer Ther Oncol* 2013; **1**:01016.
 29. Rana SB. Dose prediction accuracy of anisotropic analytical algorithm and pencil beam convolution algorithm beyond high density heterogeneity interface. *South Asian J Cancer* 2013; **2**:26-30.
 30. Ojala J. The accuracy of the Acuros XB algorithm in external beam radiotherapy – a comprehensive review. *Int J Cancer Ther Oncol* 2014; **2**:020417.
 31. Lu L. Dose calculation algorithms in external beam photon radiation therapy. *Int J Cancer Ther Oncol* 2013; **1**:01025.